

# Unsteady FW-H simulation of aerodynamic noise of a high speed train bogie

Martin Rissmann<sup>1</sup>, Romain Leneveu  
Vibratec – Railway Business Unit,  
28 Chemin du Petit Bois, 69130 ECULLY Cedex, France

Claire Chaufour<sup>2</sup>, Alexandre Clauzet, Fabrice Aubin  
SNCF Voyageurs – Centre d'ingénierie du matériel,  
4, Allée des Gémeaux, 72100 Le Mans, France

## ABSTRACT

*Aerodynamic noise is generated by interaction of the air flow with an object and by the turbulent flow itself. In railways it becomes a significant noise source for speeds above 250 kph and major areas of noise generation on trains, in particular high speed trains, are the train head, the leading and second bogie, the pantograph and the gaps between trailers. This paper presents a numerical simulation approach based on CFD/CAA techniques aiming to predict aerodynamic noise of different components of SNCF's TGV high speed trains. The approach is based on an unsteady DES flow simulation combined with the Ffowcs-Williams and Hawkins (FW-H) analogy for the acoustic part. In order to develop the method different models are implemented and the leading bogie was selected as an application case. A simplified symmetric model will be compared against a full, higher resolved model in order to see if computation time gains are feasible. Results of this simulation, in terms of sound power and directivity, are already used by SNCF noise experts in order to estimate pass-by noise levels of TGV high speed trains at the noise emission point.*

## 1. INTRODUCTION

Railway noise is largely dominated by rolling noise. However, above 250 to 300 kph and beyond, the aerodynamic noise becomes a significant additional source, which can even become the dominant noise source. It is characterized by an evolution with speed following 60 to 80 log laws and its tonal and broadband character in the low and mid-frequency range [1]. The noise is generated by interaction of the air flow with the train surfaces and by the turbulent flow itself (turbulent boundary layer, unsteady wake, etc.). It is well known from several publications [2], [3] and [4] that the major aerodynamic noise sources are the train head, the leading and second bogie, the pantograph and the gap between trailers.

For SNCF the main goal is to be able to characterize aerodynamic noise sources in order to include them in exterior noise emission predictions at train level (including rolling and equipment noise sources) for typical EMU running at 200 kph and more. Furthermore once the noise emission of the whole train is simulated, SNCF is able to define the source term for the CNOSSOS noise assessment method (European parliament directive 2002/49/CE).

Determining aerodynamic noise of high speed trains by numerical simulation is documented in several literature sources: [5] studies for example the impact of different streamlined train heads with a LES/FW-H/APE method. The noise of the entire trainset is predicted. [6] considers a simplified ICE3 high-speed train model to study noise generated at the front part of the train. The bogie is however omitted in this study. [7] focuses on the noise generation at the bogie. A simplified, isolated bogie is considered.

The presented work is focused on developing a numerical simulation approach based on CFD/CAA techniques aiming to predict aerodynamic noise of different areas of SNCF's TGV high

---

<sup>1</sup> martin.rissmann@vibratec.fr

<sup>2</sup> claire.chaufour@sncf.fr

speed trains. In order to develop the method different models are implemented and the leading bogie was selected as an application case.

## 2. METHODOLOGY

SNCF uses STARCCM+ for different aerodynamic simulations. Therefore in this study, this tool is used for the prediction of the aerodynamic sound power of the leading bogie. The prediction approach is based on an unsteady DES flow simulation combined with the Ffowcs-Williams and Hawkins (FW-H) analogy for far-field acoustic prediction. To ensure a correct implementation of the approach in STARCCM+ the well-known reference case of flow noise around a tandem cylinder was reproduced before modelling the TGV train: Satisfying agreement with the simulated and measured reference case was obtained [8].

### 2.1. Setup

Figure 1 shows the computation domain with the TGV train's head: the nose is placed far from the inlet boundary condition such that the flow field develops properly. The bogie geometry is modelled in detail including suspension elements, brake discs, motors and gearboxes. After the first bogie the train's geometry is simplified by extruding its section up to the outlet boundary condition. Furthermore, a symmetry plane is introduced along the centre axis of the train to save computation time. This hypothesis is acceptable with regard to the objective of the project. A model taking into account the full geometry is currently in work.

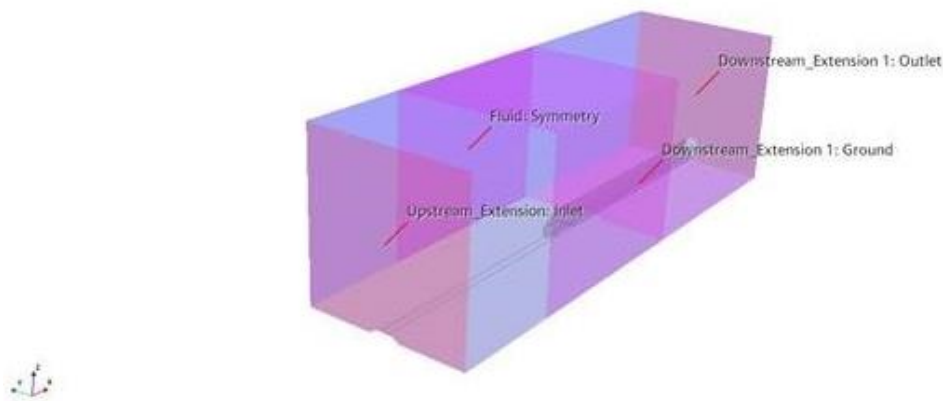


Figure 1 – Computation domain and boundaries – X = longitudinal, Y = lateral, Z = vertical

The mesh, in total 36 million trimmed cells, is gradually refined from 0.56 m towards the bogie area, where a cell size of 17.5 mm is reached, see Figure 2. More details about the mesh parameters and the boundary conditions are given in Table 1 and 2. The chosen mesh resolution allows to solve turbulence up to 500 Hz (local turbulent fluctuations compared to mesh size), respectively 1000 Hz for the acoustic part (at least 20 elements per wavelength).

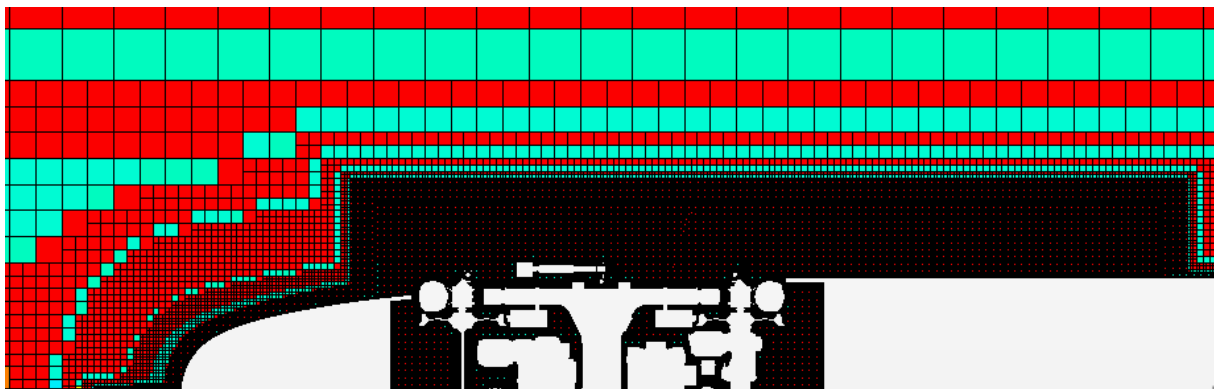


Figure 2 – Computation mesh in a horizontal plane 1.5 m above ground

Table 1 – Mesh parameters

Parameter	Value
Domain length (X)	20 m upstream extension + 37.75 m + 40 m downstream extension
Domain width (Y)	10 m
Domain height (Z)	25 m
Boundary layers	6
1 <sup>st</sup> layer thickness	2e-5 m
Boundary layer thickness	4.4 mm

Table 2 – Boundary conditions

Boundary	Value
Inlet	Velocity inlet 320 km/h
Outlet	Pressure outlet
Ground	Wall - no slip
Sides	Symmetry
Y = 0	Symmetry

## 2.2. FW-H

The sound pressure at far-field receivers is predicted using the FW-H acoustic analogy with Farrassat's Formulation 1A. Two FW-H source regions are defined: The first one, so called impermeable surface, takes into account the skin of the bogie, which corresponds to free-field radiation, see Figure 3 left. The second one, is a so-called permeable surface allowing to take into account acoustic interaction in the bogie cavity, see Figure 3 right. The back surface in downstream direction of this FW-H is not considered in the evaluation since it is known that artificial, spurious signals might appear [9]. The mesh size in the permeable FW-H is 8.4 mm, which makes this region computationally expensive. FW-H volume terms (quadrupole noise), which take into account nonlinearities in the flow and are computationally expensive, are not considered.

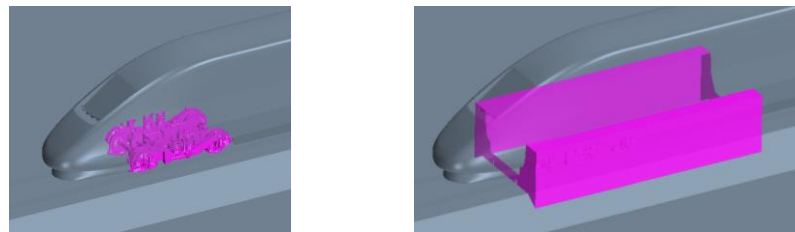


Figure 3 – left: Impermeable FW-H surface – right: permeable FW-H surface

## 2.3. Numerical resolution

The numerical resolution of the problem consists of three steps: First the flow field is initialized with a steady RANS model. Then, in the second step, the unsteady flow field, resolved by a DES model, is initiated in order to develop the turbulent flow ( $\Delta t = 1^e-3$  s up to physical time  $t = 0.5$  s) before activating in the third step the FW-H model with a time step of  $\Delta t = 6.5^e-5$  s.

Pressure signals at virtual microphone positions are recorded at a frequency of 5.1 kHz starting from 0.6 s physical time. Further details of the resolution approach are given in Table 3. The chosen approach is aggressive since only one flow flush between the train nose and the end of the bogie zone (estimated time 0.09 s) is considered before starting signal recording. This choice is made in order to meet the major aim of the project which consisted in implementing the complete modelling approach up to the equivalent noise source.

Table 3 – Model and solver parameters

Parameter	Value
Turbulence	K-Omega SST
Gas	Ideal Gas
Solver	Segregated Flow & Fluid Temperature
Numerical scheme	2 <sup>nd</sup> order implicit
Iterations per times step	min. 5 – max. 10

## 2.4. Post-processing

For each virtual microphone pressure signals are either recorded directly (FW-H on the fly) or in a post-FW-H approach for a duration of 0.125 s. For the later, the necessary flow field data is exported during the computation run. This approach has the advantage that microphone positions do not have to be defined beforehand.

The equivalent acoustic source of the bogie is described by the sound power and directivity which are both determined using a virtual microphone array, see Figure 4. The sound power is obtained from the mean pressure of 40 microphones arranged regularly on a hemisphere around the bogie centre (ISO 3745 standard). The pressure signals from the modelled side are mirrored to the non-modelled, symmetric side. Furthermore, ground effects are not considered.

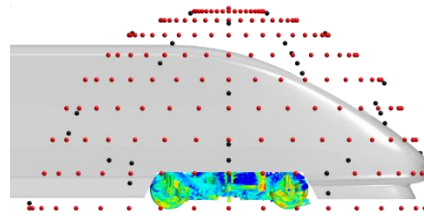


Figure 4 – Virtual microphone array used to determine the equivalent acoustic source of the bogie

## 3. RESULTS

### 3.1. Flow field

The aerodynamic part of the model is validated by comparing the drag force to results obtained previously by a numerical simulation with Powerflow [10]. A good agreement is observed such that the model is validated from this point of view.

A snapshot of the instantaneous velocity field in the bogie area, see Figure 5, reveals the turbulent nature of the flow: First the flow is slowed down up to the stagnation point at the nose, before being accelerated below the car body. Strong flow-structure interaction, mainly observed at the axle box of the first wheelset and the longitudinal damper, causes formation of turbulent eddies combined with strong velocity gradients.

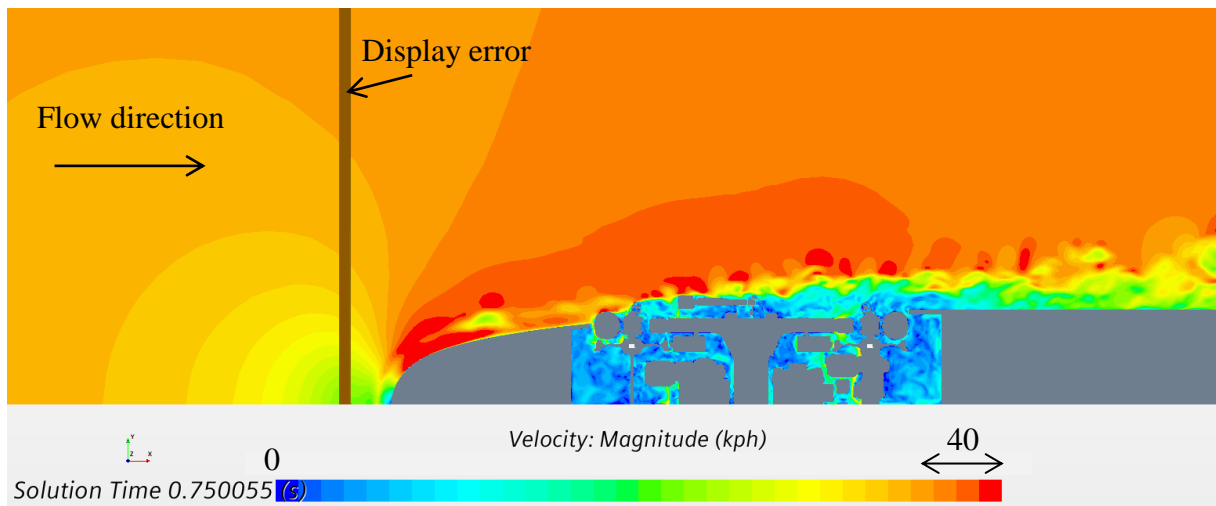


Figure 5 – Instantaneous pressure fluctuations  $p'$  in a horizontal plane 1.5 m above ground

Aerodynamic noise sources are related to instantaneous pressure fluctuations  $p' = p - \bar{p}$  as shown in Figure 6. The main fluctuations in the shown plane are located at the previously identified regions of strong flow-structure interaction, see Figure 5: The axle box of the first wheelset and the longitudinal damper are both elements that protrude above the car body envelope.

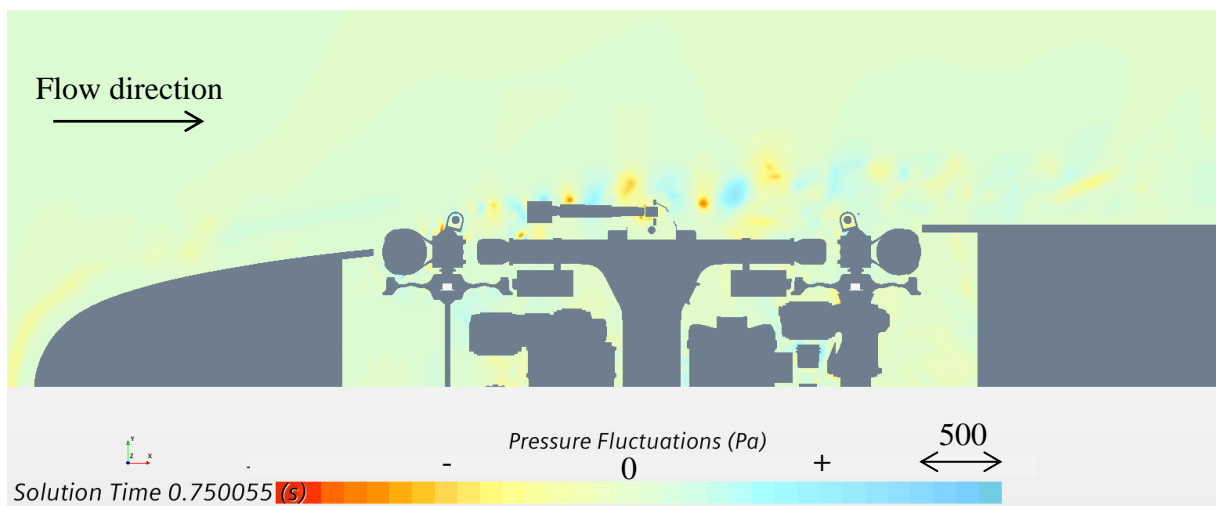


Figure 6 – Instantaneous pressure fluctuations  $p'$  in a horizontal plane 1.5 m above ground

### 3.2. Acoustics

Figure 7 shows the sound power spectra of the two FW-H source regions: taking into account the bogie cavity (permeable region) leads to a 5 dB lower noise level. Furthermore the spectra reveal two emerging third octave bands at 250 and 500 Hz third octave band, which are probably related to flow-structure interaction in the region of the axle box and longitudinal damper (see Figures 5 and 6). Both bands were previously observed by SNCF in numerical simulations and measurement campaigns, so the results of this work can be trusted.

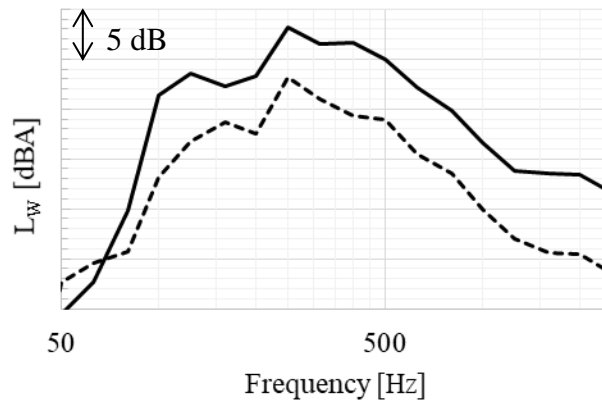


Figure 7 – Sound power – full line: impermeable FW-H source – dashed line: permeable FW-H source

Figure 8 shows the directivity patterns in horizontal direction of both FW-H sources in the 250 Hz third octave band. The directivity from the modelled side is mirrored to the non-modelled side. The leading bogie has a dipole radiation characteristic in the horizontal plane.

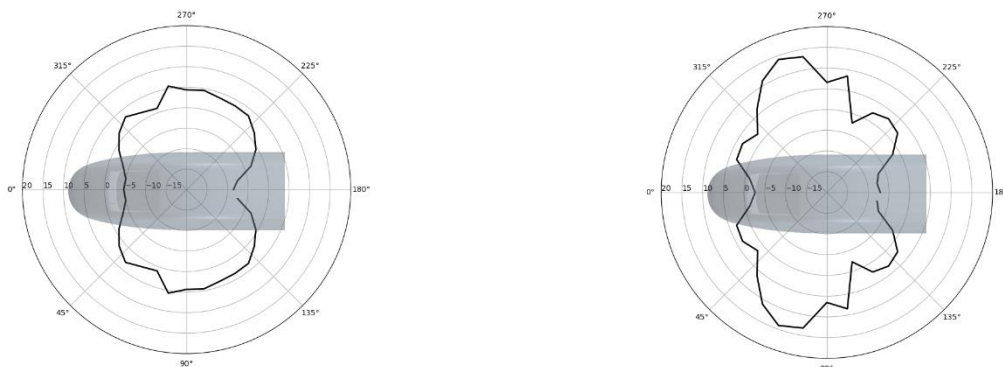


Figure 8 – Horizontal directivity [dB] in the 250 Hz band of the symmetric model – Left: Impermeable FW-H source surface – Right: Permeable FW-H source surface

#### 4. CONCLUSIONS

In this work a numerical simulation approach based on CFD/CAA techniques is developed to predict aerodynamic noise of different components of SNCF's TGV high speed trains. The approach is applied to estimate an equivalent acoustic source for the first, leading bogie. First results, obtained with a symmetric, computationally less expensive model are presented. The results reveal that the leading bogie has a dipole characteristic with emerging frequencies in the 250 and 500 Hz third octave band, which was also observed in previous works by SNCF. Using two different FW-H source zones allow to show the bogie cavity acts as an acoustic screen and influences the source directivity.

In a next step, the results will be compared to a higher resolved model which also takes into account the complete geometry allowing to validate the computationally less expensive symmetric approach. In the future the suggested approach will allow SNCF to estimate other aerodynamic noise sources such as the pantograph recess, the inter coach gap and the second bogie for example. Also, the impact of noise mitigation devices such as flow deflectors can be quantified before actual prototype tests.

Finally, the results from this work are already used by SNCF noise experts in order to predict the exterior noise emission of TGV high speed trains.

## 6. REFERENCES

1. D. Thompson, Railway noise and vibration: mechanisms, modelling and means of control, *Elsevier*, 2008.
2. C. Mellet, F. Létourneaux, F. Poisson, C. Talotte, High speed train noise emission: Latest investigation of the aerodynamic/rolling noise contribution. *Journal of sound and vibration*, 293(3-5), 535-546, 2006.
3. F. Poisson, Railway noise generated by high-speed trains, *Proceedings of the 11th International Workshop on Railway Noise*, Uddevalla, 2013.
4. J. Zhang et al., Source contribution analysis for exterior noise of a high-speed train: experiments and simulations, *Shock and Vibration*, 2018.
5. C. Li, Y. Chen, S. Xie, X. Li, Y. Wang, Y. Gao, Evaluation on Aerodynamic Noise of High Speed Trains with Different Streamlined Heads by LES/FW-H/APE Method, *Noise and Vibration Mitigation for Rail Transportation Systems*, pp. 57-65, Springer, 2021
6. G. Minelli, H. D. Yao, N. Andersson, N. P. Höstmad, J. Forssén, S. Krajnović, An aeroacoustic study of the flow surrounding the front of a simplified ICE3 high-speed train model. *Applied Acoustics*, 160, pp. 107-125, 2020.
7. E. L. Iglesias, D. J. Thompson, M. G. Smith, Component-based model for aerodynamic noise of high-speed trains. In *Noise and Vibration Mitigation for Rail Transportation Systems*, pp. 481-488, Springer, 2015.
8. D. Lockard, Summary of the tandem cylinder solutions from the benchmark problems for airframe noise computations-I workshop. *49th AIAA Aerospace Sciences Meeting including the New Horizons Forum and Aerospace Exposition*, p. 353, 2011.
9. L. V. Lopes et al., Identification of Spurious Signals from Permeable Ffowcs-Williams and Hawkings Surfaces, *American Helicopter Society (AHS) International Annual Forum and Technology Display*, No. NF1676L-25336, 2017
10. E. Masson, N. Paradot, E. Allain, The Numerical Prediction of the Aerodynamic Noise of the TGV POS High-Speed Train Power Car, *Proceedings of the 10th International Workshop on Railway Noise*, Nagahama, 2010